BULLETIN OF THE POLISH ACADEMY OF SCIENCES
TECHNICAL SCIENCES, Vol. 73(4), 2025, Article number: e154206
DOI: 10.24425/bpasts.2025.154206

SPECIAL SECTION

A flying start method for sensorless induction machine-based electric drives

Daniel WACHOWIAK*

Department of Electric Drives and Energy Conversion, Faculty of Electrical and Control Engineering and EkoTech Center, Gdansk University of Technology, ul. Narutowicza 11/12, 80-233 Gdańsk, Poland

Abstract. This paper presents an analysis of a proposed flying start method for sensorless electric drives based on an induction machine. The method introduces two stages. In the first stage, the rotor speed is estimated using the step response of the machine, which enables coarse estimation of the speed and direction of rotation, helping to reduce the initial slip. The second stage introduces an intermediate control system to facilitate the machine restart and assist the speed observer in converging. Simulation and experimental studies demonstrate that the method successfully restarts the machine with an unknown initial rotor speed without exceeding the nominal current. The auxiliary control system fully excites a 5.5 kW machine within 300 ms during the flying start, after which it is possible to transition to the target control system.

Keywords: induction machine; flying start; speed observer; sensorless drive; DC injection.

NOMENCLATURE

$\overline{}$	Vector quantity
i_s, i_r	Stator and rotor current
i_{sd}, i_{sq}	Stator current compounds in the rotating reference frame fixed to the rotor flux
$i_{s\,\max}$	Maximum stator current during restart procedure
ψ_s, ψ_r	Stator and rotor flux
$\psi_{r\,\max}$	Maximum rotor flux during restart procedure (limited by $i_{s\,\max}$)
u_s	Stator voltage
$\breve{u}_s$	Initial stator voltage during restart procedure
$u_{sx\,\max}$	Maximum stator voltage during initial speed estimation (limited by $i_{s\,\max}$)
ω_r	Rotor speed
$\breve{\omega}_r$	Rotor speed estimated during initial speed estimation
$\tilde{\breve{\omega}}_r$	Initial rotor speed estimation error
ω_s	Stator voltage vector frequency
s	Slip
$s_{\max}$	Maximal slip without exceeding maximal stator current and nominal rotor flux
R_s, R_r	Stator and stator resistance
L_s, L_r	Stator and rotor inductance
L_m	Magnetizing inductance
$k_{\psi sy/usx}$	Static gain (ψ_{sy}/u_{sx}) during initial speed estimation

1. INTRODUCTION

In many applications, electric drives can experience sudden shutdowns due to factors such as power loss or overcurrent faults. In this case, immediate restart of the drive can be problematic due to non-zero rotor speed, especially in high inertia setups where the rotor can spin for minutes before stopping. Other common cases where the machine may spin during startup include moving electric vehicles, fans, wind turbines, and water pumps that are driven by external force. Restarting an electric drive under these conditions is called a flying start.

Starting an induction machine with a high initial slip frequency caused by an unknown rotor speed can result in a high inrush current, which can cause an overcurrent fault and fail the restart procedure. Speed-sensing can facilitate flying start by reducing slip, but in some applications, sensorless solutions may be a better approach. The absence of an encoder sensor reduces the overall cost of the drive, which is particularly noticeable in low-power applications, and eliminates installation issues as well as increases reliability, especially in dusty environments. Sensorless control strategies can also be used as an emergency control system in the event of sensor failure, where high dependability is required.

The estimation of speed for unpowered permanent-magnet synchronous machines (PMSM) is possible through the utilization of the back electromotive force (EMF) signal [1–4]. In the case of a cage induction machine (IM), the back EMF decays relatively quickly after power loss, rendering methods suitable for PMSM inapplicable to IM. The sensorless flying start problem for IM may be solved by frequency search methods [5–7], where the stator is fed with a high-frequency voltage and then the frequency is reduced until zero input power, hence zero slip, is detected. A different method utilizes fuzzy logic control to adjust the stator voltage frequency and limit the inrush current [8]. The main advantage of the presented methods is that they do not require additional hardware components compared to methods that require a voltage-sensing circuit [9]. Another approach is dc current injection-based methods [1, 10, 11]. A step response of an induction machine contains oscillations with a frequency

*e-mail: daniel.wachowiak@pg.edu.pl

Manuscript submitted 2024-10-01, revised 2025-02-22, initially accepted for publication 2025-03-21, published in July 2025.

proportional to the rotor speed. By measuring this frequency, an initial speed estimate can be obtained in a relatively short time and without additional hardware.

Modern electric drives often implement advanced vector control systems. Such systems require information about the position of the flux vector, which is not an easily measurable quantity. In practice, estimators are employed to obtain flux vectors [12]. More complex observers can be implemented in order to obtain rotor speed as well, which can be used in sensorless drives [13–16]. However, in such cases, the estimated values are not available during the flying start phase and the vector control systems may fail to restart the machine. This paper proposes a flying start strategy for sensorless drives with vector control systems. The introduction of a temporary control system is proposed as a method to settle the observer and reduce slip to zero within a short period while ensuring that the nominal current is not exceeded. Furthermore, a method for initial rotor speed estimation based on DC injection in the free-running machine is proposed to reduce initial slip. Unlike the methods described in [1, 10, 11], the proposed approach examines the static gain of the IM rather than the frequency of the current oscillations during the transient state. In low-power machines, the time constants of the drive may be shorter than in high-power machines, leading to a fast decay of the oscillatory component of the output. In such cases, determining the frequency of the current oscillations can be difficult. The method proposed in this paper, based on static gain, works well even when no oscillations are present in the step response.

2. INDUCTION MACHINE MODEL

The following mathematical model of an induction machine is assumed in this paper:

$$\frac{\mathrm{d}\bar{\psi}_s}{\mathrm{d}t} + R_s\bar{i}_s = \bar{u}_s\,, \tag{1}$$

$$\frac{\mathrm{d}\bar{\psi}_r}{\mathrm{d}t} - \mathrm{j}\omega_r\bar{\psi}_r + R_r\bar{i}_r = \bar{0}\,, \tag{2}$$

$$\bar{\psi}_s = L_s\bar{i}_s + L_m\bar{i}_r\,, \tag{3}$$

$$\bar{\psi}_r = L_r\bar{i}_r + L_m\bar{i}_s\,, \tag{4}$$

where ψ_s, ψ_r are stator and rotor flux, i_s, i_r are stator and rotor current, ω_r is rotor speed, R_s, R_r are stator and rotor resistances, L_s, L_r, L_m are stator, rotor, and magnetizing inductances. Symbol - denotes vector quantities.

The equation set (1)–(4) can be rewritten with i_s and ψ_s as state variables

$$\frac{\mathrm{d}x}{\mathrm{d}t} = Ax + Bu, \tag{5}$$

$$y = Cx, \tag{6}$$

where

$$x = \begin{bmatrix} i_{sx} & i_{sy} & \psi_{sx} & \psi_{sy} \end{bmatrix}^T, \tag{7}$$

$$u = \begin{bmatrix} u_{sx} & u_{sy} \end{bmatrix}^T, \tag{8}$$

$$A = \begin{bmatrix} -\dfrac{R_sL_r + L_sR_r}{w}I + \omega_r J & \dfrac{R_r}{w}I - \dfrac{\omega_r L_r}{w}J \\ -R_sI & 0 \end{bmatrix}, \tag{9}$$

$$B = \begin{bmatrix} \dfrac{L_r}{w}I \\ I \end{bmatrix}, \tag{10}$$

where subscripts x, y denote compounds of the vectors and

$$I = \begin{bmatrix} 1 & 0 \\ 0 & 1 \end{bmatrix}, \tag{11}$$

$$J = \begin{bmatrix} 0 & -1 \\ 1 & 0 \end{bmatrix}, \tag{12}$$

$$w = L_sL_r - L_m^2\,. \tag{13}$$

3. FLYING START ALGORITHM

It is necessary to supply power to the induction machine for the speed observer to estimate state variables. If the nominal stator voltage is supplied when the rotor speed is unknown, this may result in a high slip, which will in turn cause a high stator current. The objective of the proposed flying start method is to limit the current to a value close to its nominal value $i_{s\,\max}$.

In accordance with the mathematical model of the induction machine presented in Section 2, the stator current compound i_{sd} and slip s can be expressed as follows:

$$i_{sd} = \frac{\psi_r}{L_m}\,, \tag{14}$$

$$s = R_r\frac{L_m}{L_r}\frac{i_{sq}}{\psi_r}\,, \tag{15}$$

where i_{sd} and i_{sq} are the compounds of stator current in the rotating reference frame fixed to the rotor flux. With the constraint on stator current

$$i_{sd}^2 + i_{sq}^2 \le i_{s\,\max}^2\,, \tag{16}$$

the maximum rotor flux that can be achieved without exceeding the maximal current can be computed from the following formula:

$$\psi_{r\,\max} = \frac{R_rL_m i_{s\,\max}}{\sqrt{R_r^2 + L_r^2 s^2}}\,. \tag{17}$$

As illustrated in Fig. 1, rotor flux decreases rapidly when slip increases. If an arbitrary rotor speed is assumed during the flying start, it may cause a high slip. As a result, when the stator voltage is reduced to keep the stator current within limits, the rotor flux becomes low. In such circumstances, the speed observer is susceptible to parameter errors, and the accuracy of estimation may be inadequate.

Figure 2 presents the general algorithm of the flying start procedure. It is recommended that the machine be started with

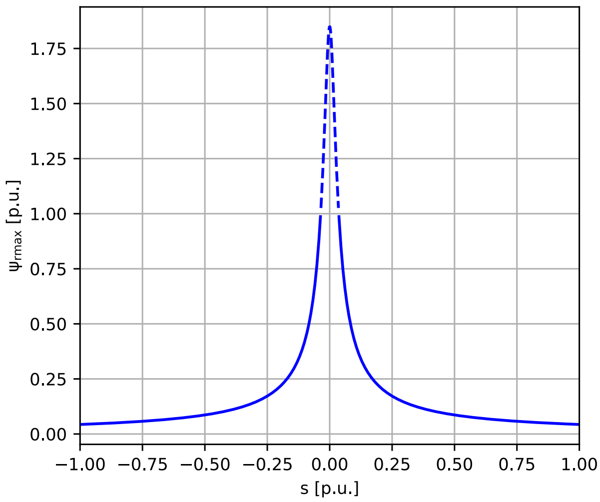

Fig. 1. Rotor flux in function of slip at nominal stator current for machine parameters presented in the Appendix

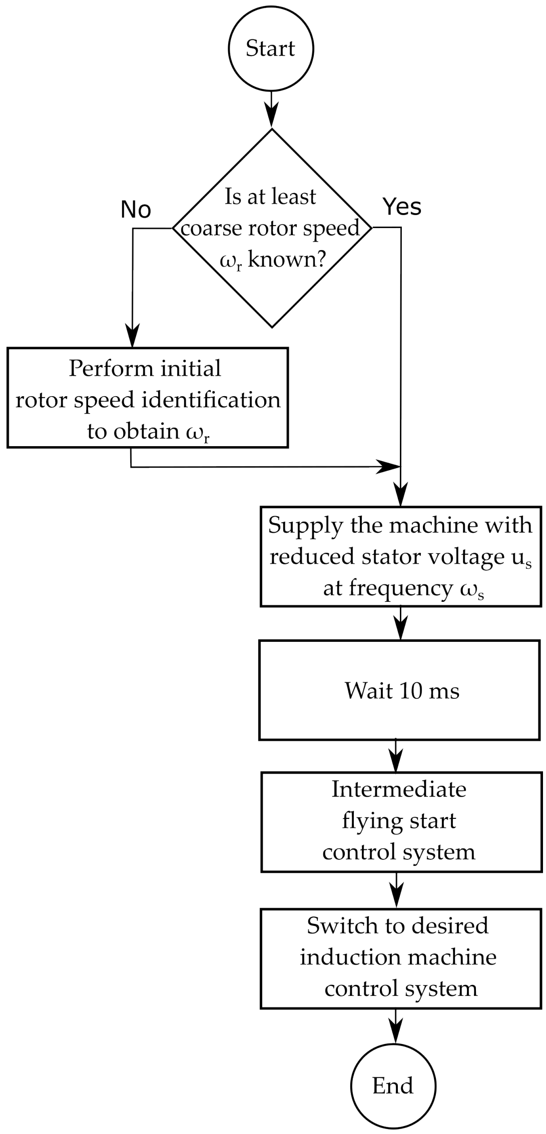

Fig. 2. Block diagram of the flying start procedure

a stator voltage frequency as close to the real rotor speed as possible to reduce the slip and ensure that the rotor flux is high enough to provide the desired speed observer accuracy. In certain circumstances, the coarse rotor speed ω_s may be known (e.g., following a system restart, when the previous rotor speed was memorized and the restart occurred shortly after the shutdown, or when the system is equipped with sensors that may assist in estimating the rotor speed, such as a flow meter in the case of water pumps). In the absence of rotor speed information, an initial speed estimation method presented in Section 4 may be employed.

In the next step, the motor is supplied with a stator voltage at frequency ω_s and a reduced value to prevent overcurrent. At this point, the speed observer begins estimating variables. It is advisable to allow the observer to settle for about 25 milliseconds before proceeding to the next step to avoid negative impacts on the control system from oscillations in estimated values during the transient state of the observer. Due to the reduced stator voltage, the rotor flux may still be significantly below the nominal value, which makes the speed observer prone to model inaccuracies or measurement errors. A flying start control system, described in Section 5, is proposed to facilitate the convergence of the observer. Once the procedure is complete, the accuracy of the estimation allows for switching to the target control system of the induction machine.

4. INITIAL ROTOR SPEED ESTIMATION

The initial rotor speed estimation method proposed in this paper is based on the analysis of the step response of the induction machine. The steady-state values of the state variables can be used to predict the rotor speed. The static gains of the system (5) are shown in Table 1, with stator voltage vector compounds as an input and stator current or stator flux as an output.

Table 1
Static gains of induction machine

Out \ In	u_{sx}	u_{sy}
i_{sx}	$\frac{1}{R_s}$	0
i_{sy}	0	$\frac{1}{R_s}$
ψ_{sx}	$\frac{R_r^2 L_s + \omega_r^2 L_r w}{R_s R_r^2 + \omega_r^2 L_r^2 R_s}$	$\frac{R_r \omega_r (w + L_r L_s)}{R_s R_r^2 + \omega_r^2 L_r^2 R_s}$
ψ_{sy}	$-\frac{R_r \omega_r (w + L_r L_s)}{R_s R_r^2 + \omega_r^2 L_r^2 R_s}$	$\frac{R_r^2 L_s + \omega_r^2 L_r w}{R_s R_r^2 + \omega_r^2 L_r^2 R_s}$

The static gain for stator current as an output is equal to zero or $1/R_s$, depending on the compound. Since it does not depend on the rotor speed, it is impossible to estimate the speed based on the steady-state value of the stator current. In contrast, the static gain for stator flux as an output depends on the rotor speed. Figure 3 shows the relationship between stator flux and stator voltage in a steady state for both compounds of the stator flux vector.

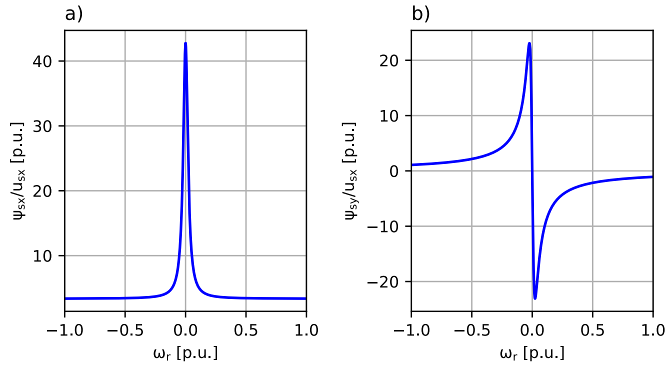

Fig. 3. Static gain of induction machine for stator voltage compound u_{sx} as an input and stator flux compounds a) ψ_{sx} and b) ψ_{sy} as an output in function of rotor speed

For high speeds, above 0.3, the steady-state compound ψ_{sx} is nearly constant for different rotor speeds (Fig. 3a). This makes it challenging to determine the speed based on the static gain. Additionally, the graph is symmetrical about the axis of ordinates, which makes it impossible to conclude the direction of rotation. In the case of compound ψ_{sy} (Fig. 3b), the value of the flux in a steady state undergoes a notable change even at high speeds, and the sign of the static gain is opposite to that of the rotor speed. This indicates that it may be feasible to determine the direction of rotation and estimate the speed by analyzing the step response in the steady state of an induction machine with u_{sx} as an input and ψ_{sy} as an output.

The value of u_{sx} must be determined in such a way as to maintain the current within the nominal value. Since the stator voltage is the product of stator current and stator resistance in the steady state (as can be concluded from Table 1), for the maximal stator current $i_{s\max}$, the maximal stator voltage $u_{sx\max}$ during initial speed estimation is

$$u_{sx\max} = kR_s i_{s\max}, \tag{18}$$

where $k \in (0, 1)$. The formula ensures that the current remains within the nominal value in the steady state. However, in the transient state, oscillations and overshoot may occur, necessitating a gain k that is less than 1.

The conversion of the static gain $k_{\psi sy}/u_{sx}$ from Table 1 allows the computation of rotor speed via the following formula:

$$\breve{\omega}_r = \frac{R_r\left(w + L_r L_s\right)}{2k_{\psi sy/usx} L_r^2 R_s} + \frac{\sqrt{R_r^2\left(w + L_r L_s\right)^2 + 4\left(k_{\psi sy/usx} L_r R_s R_r\right)^2}}{2k_{\psi sy/usx} L_r^2 R_s}. \tag{19}$$

In a typical sensorless drive, the only measured quantity is the stator current. In order to determine the static gain $k_{\psi sy}/u_{sx}$, it is necessary to estimate the stator flux. The stator flux can be computed from equation (1) by transforming it

$$\psi_{sy} = \int \left(-R_s i_{sy} + u_{sy}\right) \mathrm{d}t + \psi_{sy0}, \tag{20}$$

where ψ_{sy0} is the initial stator flux. As the value of the stator flux is unknown at the initial stage of the flying start procedure, it is advisable to apply zero stator voltage to the machine to zero the stator flux. Subsequently, during the initial estimation of rotor speed, the stator current is integrated in accordance with the formula (20) to obtain $k_{\psi sy}/u_{sx}$.

5. FLYING START CONTROL SYSTEM

It should be noted that the rotor speed obtained through the initial speed estimation method described in the previous section may be subject to error. Consequently, after applying the stator voltage at the frequency resulting from the assumed initial speed, slip will occur. The slip is equal to the initial rotor speed estimation error $\tilde{\breve{\omega}}_r$. Equation (17) can be transformed into a formula that allows for the determination of the maximal slip at which it is possible to achieve nominal rotor flux without exceeding current $i_{s\max}$

$$|s_{\max}| \leq \frac{R_r}{L_r}\sqrt{L_m^2 i_{s\max}^2 - \psi_{rn}^2}. \tag{21}$$

Applying too high a stator voltage during flying start may result in overcurrent or exceeding the nominal flux. If the expected maximum rotor speed error $\tilde{\breve{\omega}}_{r\max}$ is within the slip limit defined in (21), flux limitation by ensuring a constant u_s/ω_s ratio is a sufficient solution. In the other case, the initial slip is high, and current limitation must be applied. The maximum stator voltage can be simplified as the product of the maximum rotor flux and the rotor speed. The maximum rotor flux can be expressed as (17). At low rotor speed and high slip, the electromotive force may be low, so the voltage drop across the stator resistance has been included, as it may not be negligible. Finally, the initial stator voltage $\breve{u}_s$ can be expressed as

$$\breve{u}_s = \begin{cases} \breve{\omega}_r & \text{for } \left|\tilde{\breve{\omega}}_{r\max}\right| < |s_{\max}|, \\ \breve{\omega}_r \dfrac{R_r L_m i_{s\max}}{\sqrt{R_r^2 + L_r^2 \tilde{\breve{\omega}}_{r\max}^2}} + R_s i_{s\max} & \text{for } \left|\tilde{\breve{\omega}}_{r\max}\right| \geq |s_{\max}|. \end{cases} \tag{22}$$

After the machine is supplied, the observer starts to estimate the variables, but high errors are expected due to the low flux, and it is not recommended to switch to the target control system, especially when vector control strategies are used. In Fig. 4, an intermediate flying start control system is proposed to help the observer converge. The outer loop ensures that the rotor flux tends to a value sufficient for the correct estimation of the state variables. Nominal flux as a reference value is a good starting point. Since flux is not measured, an observer-estimated value is used to find the control error. The inner loop is used to keep the stator current within the nominal range. As the observer converges, the frequency of the stator voltage ω_s is updated, resulting in a reduction in slip and faster excitation of the induction machine. A low-pass filter is applied to the observer outputs to reduce the effect of potentially violent fluctuations in the estimated variables during the transient state.

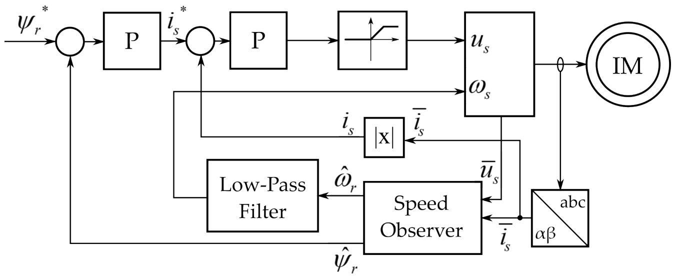

Fig. 4. Intermediate flying start control system

6. RESULTS

Studies have been conducted on a 5.5 kW induction machine, the parameters of which are presented in the Appendix (Tables 3 and 4). The investigated induction machine is coupled to a DC machine, which drives the shaft during the flying start. As the drive is assumed to be sensorless, the speed sensor is only used to calculate the estimation error.

6.1. Initial rotor speed estimation

Figures 5 and 6 show the simulation and experimental results of the initial rotor speed estimation explained in Section 4 for $\omega_r = 0.4$. The stator is supplied with a constant voltage of $u_{sx} = 0.03$ to obtain the step response without exceeding the nominal current. The stator flux is calculated from the stator current using equation (20). The static gain $k_{\psi sy}/u_{sx}$ is then transformed to rotor speed $\breve{\omega}_r$ according to equation (19). Table 2 presents the final results, including ψ_{sy}/u_{sx} gain, and the identified $\breve{\omega}_r$ for several rotor speed values, including one case with a different direction. In the experiment on the real machine, the estimation error tends to rise with rotor speed, and in the case of nominal rotor speed, the error reaches 0.16 p.u. This is a fairly large error; however, it allows for a significant reduction of initial slip and facilitates the flying start procedure. Additionally, the method facilitates the determination of the rotor speed direction. As anticipated, the error is higher for high rotor speed due to relatively small changes in static gain as a function of speed (Fig. 3) within the high-speed range.

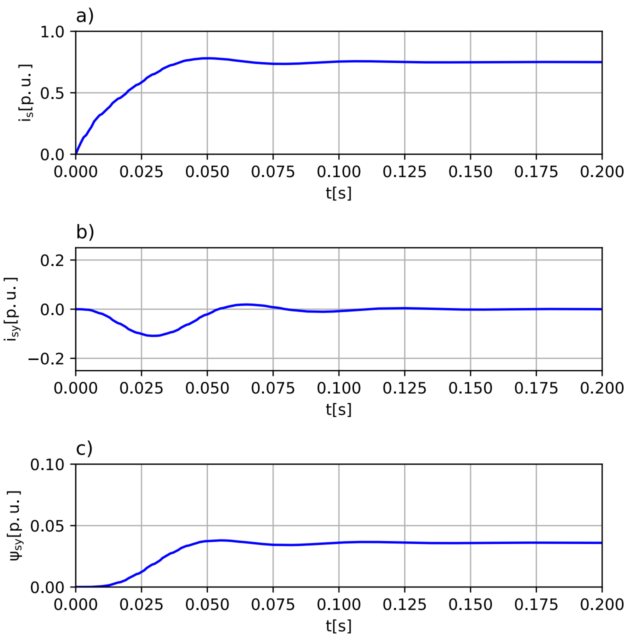

Fig. 5. Step response of the induction machine for $\omega_r = 0.4$ with $u_{sx} = 0.03$ as an input during initial rotor speed estimation – simulation results

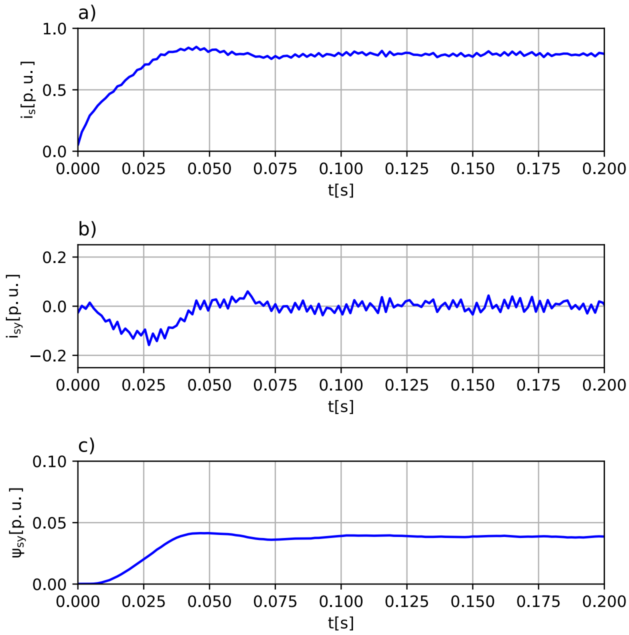

Fig. 6. Step response of the induction machine for $\omega_r = 0.4$ with $u_{sx} = 0.03$ as an input during initial rotor speed estimation – experimental results

Table 2
Accuracy of initial rotor speed estimation

ω_r [p.u.]	Simulation		Experiment	
	$k_{\psi sy}/u_{sx}$ [p.u.]	$\omega_{r\text{init}}$ [p.u.]	$k_{\psi sy}/u_{sx}$ [p.u.]	$\omega_{r\text{init}}$ [p.u.]
0.2	2.77	0.21	2.23	0.25
0.4	1.38	0.41	1.29	0.44
0.6	0.92	0.62	0.91	0.62
0.8	0.69	0.82	0.82	0.76
1.0	0.54	1.06	0.70	0.84
–0.4	–1.38	–0.41	–1.39	–0.41

6.2. Intermediate flying start control system

A study of the flying start control system was conducted using a speed observer presented in [16]. The gains of the observer were selected using a method shown in [17, 18], and the values are presented in the Appendix Table 3 and 4). The simulation results for a forced rotor speed of $\omega_r = 0.5$ are presented in Fig. 7. Previous experiments show that the initial rotor speed estimation method yields an error of up to 0.16 p.u. Therefore, it can be expected that the result of the initial rotor speed estimation $\breve{\omega}_r$ should be between 0.34 and 0.66. Assuming worst cases, two values are analyzed at the boundaries of this range, resulting in the machine being supplied with initial stator voltage at frequencies $\omega_s = \breve{\omega}_r = 0.34$ and 0.66. The amplitude of the initial voltage $\breve{u}_s$ was determined using equation (22). After the machine was fed, the frequency and amplitude of the stator voltage vector remained constant for 25 ms, allowing the observer to stabilize. While both cases result in an almost zero estimation error, it is possible that on a real machine, the observer may be affected by relatively high errors at this point. It is therefore inadvisable to implement any advanced vector control system that relies on estimated variables at this time. Instead, the control system presented in Fig. 4 is employed to help reduce potential slip and increase the flux to get more reliable results. The machine reaches full excitation after about 300 ms, but the observer settles around zero estimation error much faster, within 25 ms after the flying start control system is applied.

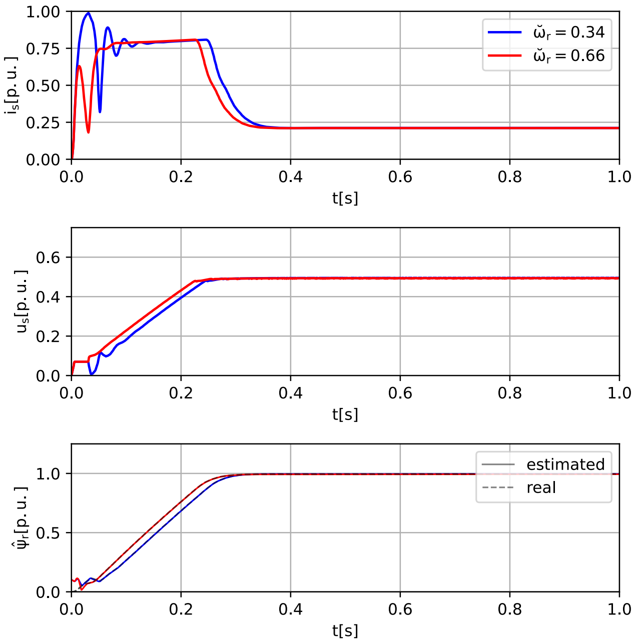

Fig. 7. Start-up of induction machine under flying start condition for $\omega_r = 0.5$ and initial rotor speed error $\tilde{\breve{\omega}}_r = \pm 0.16$ – assumed initial rotor speed $\breve{\omega}_r = 0.34$ (blue line) and 0.66 (red line)

The preceding studies were conducted under the assumption that the initial slip would fall within the initial estimation error range, which was defined as being equal to ±0.16 p.u. The results for higher errors are presented in Fig. 8. The rotor speed is $\omega_r = 0.5$, and two cases of initial rotor speed estimation are considered: $\breve{\omega}_r = 1.0$ and $\breve{\omega}_r = -0.5$. Consequently, the absolute value of the initial slip is equal to 0.5 and 1.0, respectively, with the second case assuming wrong rotation direction. In the case of $\breve{\omega}_r = 1.0$, the system initially encountered difficulties in stabilizing, but eventually reached a point of zero estimation error without exceeding the nominal current within 50 ms. In the other case the observer lost stability and the estimated rotor flux diverged to infinity, failing the restart procedure. The experiment demonstrated that the method is viable, even in the presence of relatively high initial estimation error. However, initiating the process with a slip value that is too high, or assuming an incorrect rotation direction, may result in observer instability. Consequently, it is inadvisable to assume arbitrary initial rotor speed.

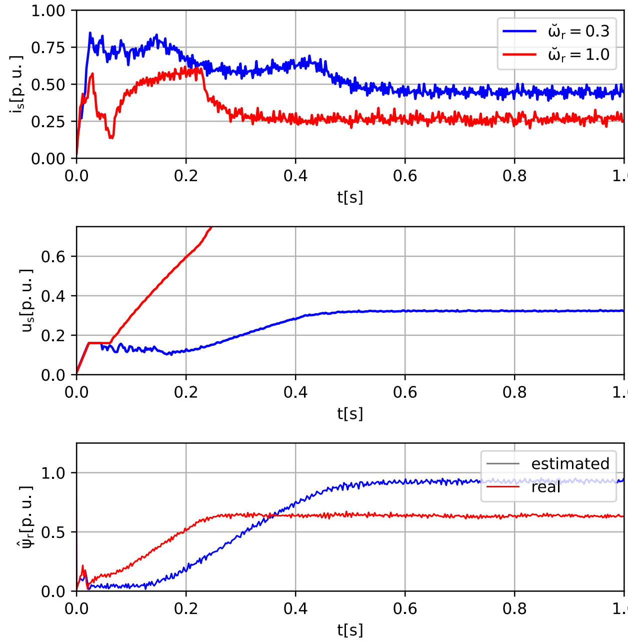

Fig. 8. Start-up of induction machine under flying start condition for $\omega_r = 0.5$ and assumed initial rotor speed $\breve{\omega}_r = 1.0$ (initial rotor speed error $\tilde{\breve{\omega}}_r = 0.5$, blue line) and $\breve{\omega}_r = -0.5$ (initial rotor speed error $\tilde{\breve{\omega}}_r = -1.0$, red line)

It is important to note that the above simulations were performed with an observer assuming zero model parameter error. Using an observer based on an exact model as the plant leads to satisfactory results, even in challenging conditions such as low flux. In reality, the precise model of the machine and the values of its parameters are unknown. This inaccuracy leads to estimation errors. These errors become especially significant when the slip is unusually high, a condition that is highly probable during a flying start. A study was conducted to demonstrate the influence of parameter errors on the observer.

The results of a simulation with a 25% error in stator and rotor resistance are shown in Fig. 9. Two cases were considered: an initial rotor speed error of 0.16 ($\breve{\omega}_r = 0.66$) and 0.5 ($\breve{\omega}_r = 1.0$). In the case of a small initial slip (within the expected boundaries of initial speed estimation), the observer converged within 100 ms. In the other case, the system failed to complete the flying start. The combination of resistance error and low flux causes significant estimation errors. Since the initial error was already high, this ultimately led to the observer failure to converge and loss of stability.

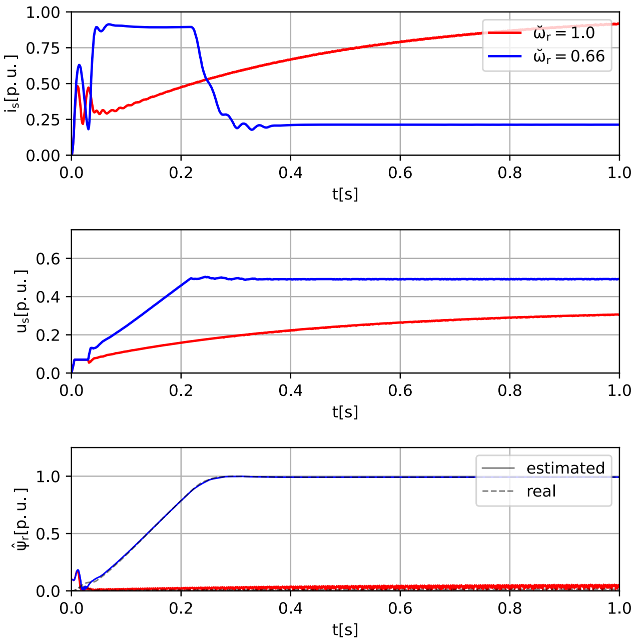

Fig. 9. Start-up of induction machine under flying start condition for $\omega_r = 0.5$, assumed initial rotor speed $\breve{\omega}_r = 1.0$(initial rotor speed

The results of verifying the simulation results on a real drive are shown in Fig. 10. Experimental studies were conducted for rotor speed values of $\omega_r = 0.3$ and $\omega_r = 1.0$. Assuming the highest initial rotor speed estimation error, the initial stator voltage frequency was calculated to be $\breve{\omega}_r = 0.46$ and $\breve{\omega}_r = 0.84$, respectively. In both cases, the observer converged and the flying start procedure was successful. For $\omega_r = 1.0$, the observer stabilized within 75 ms, while for $\omega_r = 0.3$, stabilization occurred within 175 ms.

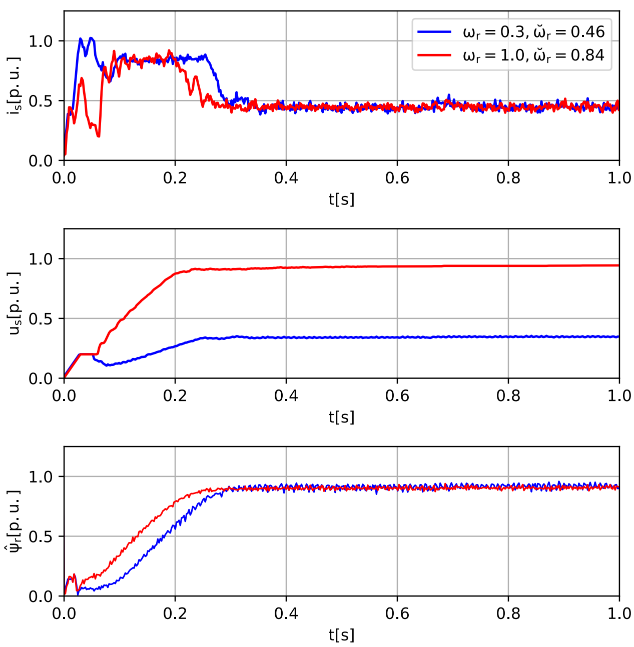

Fig. 10. Experimental results of start-up of induction machine under flying start condition for $\omega_r = 0.3$, with assumed initial rotor speed $\breve{\omega}_r = 0.46$ (blue line), and $\omega_r = 1.0$, with assumed initial rotor speed $\breve{\omega}_r = 0.84$ (red line)

7. CONCLUSIONS

In the paper, a flying start algorithm for IM is proposed. It includes a method of initial speed estimation based on the static gain of a free-running machine to determine rotation direction and estimate the coarse speed. Additionally, an intermediate control system is introduced to assist the speed observer during its transient state. The proposed methods are validated both through simulation and real experiments. The results demonstrate that the intermediate control system enables a flying start without exceeding the nominal current. Moreover, the speed observer can settle and slip is reduced to zero within 200 ms (or even faster for high rotor speeds), even before the machine is fully excited. At this stage, it is possible to switch to the target control system. The proposed method is particularly useful for advanced vector control systems that require flux estimation, as the observer is already implemented.

APPENDIX

Table 3
Parameters of the induction machine

Symbol	Quantity	Value
P_n	Nominal power	5.5 kW
U_n	Nominal stator voltage	400 V
I_n	Nominal stator current	11 A
f_n	Nominal stator frequency	50 Hz
n	Nominal rotor speed	1450 rpm
R_s	Stator resistance	0.034 p.u.
R_r	Rotor resistance	0.035 p.u.
L_m	Magnetizing inductance	2.42 p.u.
L_s	Stator inductance	2.48 p.u.
L_r	Rotor inductance	2.48 p.u.

Table 4
Observer gains

Gain	Value
k_{11}	–1.154501
k_{12}	5.095293
k_{13}	–9.375840
k_{14}	0.674525

Gain	Value
k_{21}	0.188765
k_{22}	0.408821
k_{23}	–0.832618
k_{24}	–7.730443

Gain	Value
k_{31}	–5.310812
k_{32}	–1.717221
k_{33}	–7.801986
k_{34}	–8.180284

ACKNOWLEDGEMENTS

Financial support of these studies from the Gdańsk University of Technology by the DEC-4/1/2022/IDUB/I3b/Ag grant under the ARGENTUM – "Excellence Initiative – Research University" program is gratefully acknowledged.

REFERENCES

[1] H. Iura, K. Ide, T. Hanamoto, and Z. Chen, "An Estimation Method of Rotational Direction and Speed for Free-Running AC Machines Without Speed and Voltage Sensor," *IEEE Trans. Ind. Appl.*, vol. 47, no. 1, pp. 153–160, Jan. 2011, doi: 10.1109/TIA.2010.2091670.

[2] K. Lee, S. Ahmed, and S.M. Lukic, "Universal restart strategy for high-inertia scalar-controlled PMSM drives," *IEEE Trans. Ind. Appl.*, vol. 52, no. 5, pp. 4001–4009, Sep. 2016, doi: 10.1109/TIA.2016.2581764.

[3] L. Pravica, D. Sumina, T. Bariša, M. Kovačić, and I. Čolović, "Flying start of a permanent magnet wind power generator based on a discontinuous converter operation mode and a phase-locked loop," *IEEE Trans. Ind. Electron.*, vol. 65, no. 2, pp. 1097–1106, Jul. 2017, doi: 10.1109/TIE.2017.2733453.

[4] D.W. Seo, Y. Bak, and K.B. Lee, "An Improved Rotating Restart Method for a Sensorless Permanent Magnet Synchronous Motor Drive System Using Repetitive Zero Voltage Vectors," *IEEE Trans. Ind. Electron.*, vol. 67, no. 5, pp. 3496–3504, May 2020, doi: 10.1109/TIE.2019.2914647.

[5] K. Lee, S. Lukic, and S. Ahmed, "A universal restart strategy for induction machines," in *2016 IEEE Energy Conversion Congress and Exposition (ECCE)*, IEEE, Sep. 2016, pp. 1–6. doi: 10.1109/ECCE.2016.7854802.

[6] K. Lee, S. Ahmed, and S.M. Lukic, "Universal Restart Strategy for Scalar (V/f) Controlled Induction Machines," *IEEE Trans. Ind. Appl.*, vol. 53, no. 6, pp. 5489–5495, Nov. 2017, doi: 10.1109/TIA.2017.2733497.

[7] H. Rostami Kisomi, K. Khalaj Monfared, and H. Iman-Eini, "Sensorless flying start method for starting of induction motors," in *2021 12th Power Electronics, Drive Systems, and Technologies Conference (PEDSTC)*, IEEE, Feb. 2021, pp. 1–5, doi: 10.1109/PEDSTC52094.2021.9405820.

[8] W. Hu, Z. Wu, L. Sun, and X. Cai, "Strategy for Restarting the Free-Running Induction Motor Driven by a High-Voltage Inverter Based on V/F Fuzzy Control," in *2016 8th International Conference on Intelligent Human-Machine Systems and Cybernetics (IHMSC)*, IEEE, Aug. 2016, pp. 99–102, doi: 10.1109/IHMSC.2016.77.

[9] S. Choi, J. Lee, C. Hong, and A. Yoo, "Restarting strategy for an induction machine driven with medium-voltage inverter," in *2015 9th International Conference on Power Electronics and ECCE Asia (ICPE-ECCE Asia)*, IEEE, Jun. 2015, pp. 1881–1888, doi: 10.1109/ICPE.2015.7168035.

[10] S. Yin *et al.*, "Fast restarting of free-running induction motors under speed-sensorless vector control," *IEEE Trans. Ind. Electron.*, vol. 67, no. 7, pp. 6124–6134, Jul. 2020, doi: 10.1109/TIE.2019.2934077.

[11] T. Kikuchi, Y. Matsumoto, and A. Chiba, "Fast Initial Speed Estimation for Induction Motors in the Low-Speed Range," *IEEE Trans. Ind. Appl.*, vol. 54, no. 4, pp. 3415–3425, 2018, doi: 10.1109/TIA.2018.2825292.

[12] G. Verghese and S. Sanders, "Observers for flux estimation in induction machines," *IEEE Trans. Ind. Electron.*, vol. 35, no. 1, pp. 85–94, 1988, doi: 10.1109/41.3067.

[13] H. Kubota, K. Matsuse, S. Member, and T. Nakmo, "DSP-Based Speed Adaptive Flux Observer of Induction Motor," *IEEE Trans. Ind. Appl.*, vol. 29, no. 2, pp. 344–348, 1993.

[14] T. Białoń, A. Lewicki, M. Pasko, and R. Niestrój, "Non-proportional full-order Luenberger observers of induction motors," *Arch. Electr. Eng.*, vol. 67, no. 4, pp. 925–937, 2018, doi: 10.24425/aee.2018.124750.

[15] Y. Laatra, H. Lotfi, and B. Abdelhani, "Speed sensorless vector control of induction machine with Luenberger observer and Kalman filter," *2017 4th International Conference on Control, Decision and Information Technologies, CoDIT 2017*, 2017, pp. 714–720, 2017, doi: 10.1109/CoDIT.2017.8102679.

[16] Z. Krzemiński, "Observer of induction motor speed based on exact disturbance model," *2008 13th International Power Electronics and Motion Control Conference, EPE-PEMC 2008*, 2008, pp. 2294–2299, doi: 10.1109/EPEPEMC.2008.4635605.

[17] D. Wachowiak, "Genetic Algorithm Approach for Gains Selection of Induction Machine Extended Speed Observer," *Energies (Basel)*, vol. 13, no. 18, p. 4632, Sep. 2020, doi: 10.3390/en13184632.

[18] D. Wachowiak, "A Universal Gains Selection Method for Speed Observers of Induction Machine," *Energies (Basel)*, vol. 14, no. 20, p. 6790, Oct. 2021, doi: 10.3390/en14206790.